ABCM Symposium Series in Mechatronics - Vol. 3 - pp.129-138

MODELING AND IDENTIFICATION OF FLEXIBLE STRUCTURE USING BOND GRAPHS APPLIED ON FLEXCAM QUANSER SYSTEM

Euler Gonçalves Barbosa
CTA/IAE - Instituto de Aeronáutica e Espaço
Praça Marechal Eduardo Gomes, 50, CEP 12.228-904
São José dos Campos - SP
euler@iae.cta.br

Luiz Carlos Sandoval Góes
CTA/ITA – Instituto Tecnológico de Aeronáutica
Praça Marechal Eduardo Gomes, 50, CEP 12.228-904
São José dos Campos - SP
goes@ita.br

Abstract. *The dynamic behavior of a flexible structure is similar to fluid moving (known as sloshing) in liquid-propellant rocket motors, subjected to external efforts. Thus, modeling and identification of flexible modes are similar to sloshing modes. This paper presents results from modeling using Bond-Graphs (State-Space equations and Transfer Functions) applied to an angular position servo and flexible beam used on Flexible Link FLEXCAM Quanser System, as well as results from identification process using ARX model. On first step, only angular servo position is tested, input/output time histories are recorded and submitted to identification process. As second step, the flexible structure is fixed to hub and new input/output data are collected to perform new identification with the previous model obtained on first step. The sampling frequency and a pseudo-random binary sequence (PRBS) input are discussed against previously measures of time constants and three mode frequencies. The complete model obtained from match and identification process is presented, useful to flexible mode control designs, e. g., LQR,* H_∞ *and PID strategies. The natural frequencies and damping ratios are used to design and validate a compensated inverse PID controller to damp flexible modes.*

Keywords*: Modeling, Identification, Flexible Structure, Bond-Graphs*

1. INTRODUCTION

The modeling and identification of a dynamic system (plant) is an interactive process necessary to obtain a model with good reliability. The Flexible Link FLEXCAM Quanser System is a very useful equipment to perform this, and so is presented in details. The transfer function of the hub is modeled using Bond-Graphs and its coefficients are identified using parametric identification (ARX). The next step is the modeling and identification of the flexible structure, where the Hamilton’s Principle is used to derive the equations of motion. The Bond-Graphs are developed and presented based on these equtions of motion. Specific programs are used to produce the overall transfer function, in such way, that presents the hub and flexible dynamics. The results and models obtained are thus used to design a digital controller presented in Barbosa and Góes (2007).

2. THE FLEXCAM QUANSER SYSTEM

The Quanser System is presented in Fig. 1, used to validate control strategies to Brazilian Vehicle Satellite Launcher (VLS), placed at Hybrid Simulation Laboratory (LabSI) of Institute of Aeronautics and Space (CTA-IAE).

The flexible structure (flexible link) is a uniform flexible beam mounted on the rotating servo plant (hub). The light source is attached to the tip of the beam which is detected by a camera mounted to the rotating base. The hardware and equipments of Quanser System consists of a Universal Power Module and a terminal board data acquisition. The hub is used to rotary motion experiments and consists of a DC motor mounted with a gearbox. The terminal and the Multiq boards perform the analogic to digital and digital to analogic conversion (A/D, D/A).

The software used to developing, compiling and to perform digital control consists on the Simulink, Real-Time Workshop, Watcom C++ compiler and the WinCon controller. The WinCon is a realtime program that performs the digital controller and can perform sampling frequencies less than 200Hz (T = 5ms). The figures as follow show the typical blocks used in Simulink toolbox, as closed loop control system. It can be used, with few modifications, to operate in opened or closed loops.

(a) (b)

Figure 1. (a) The FLECAM Quanser System (b) Hub, camera and flexible beam

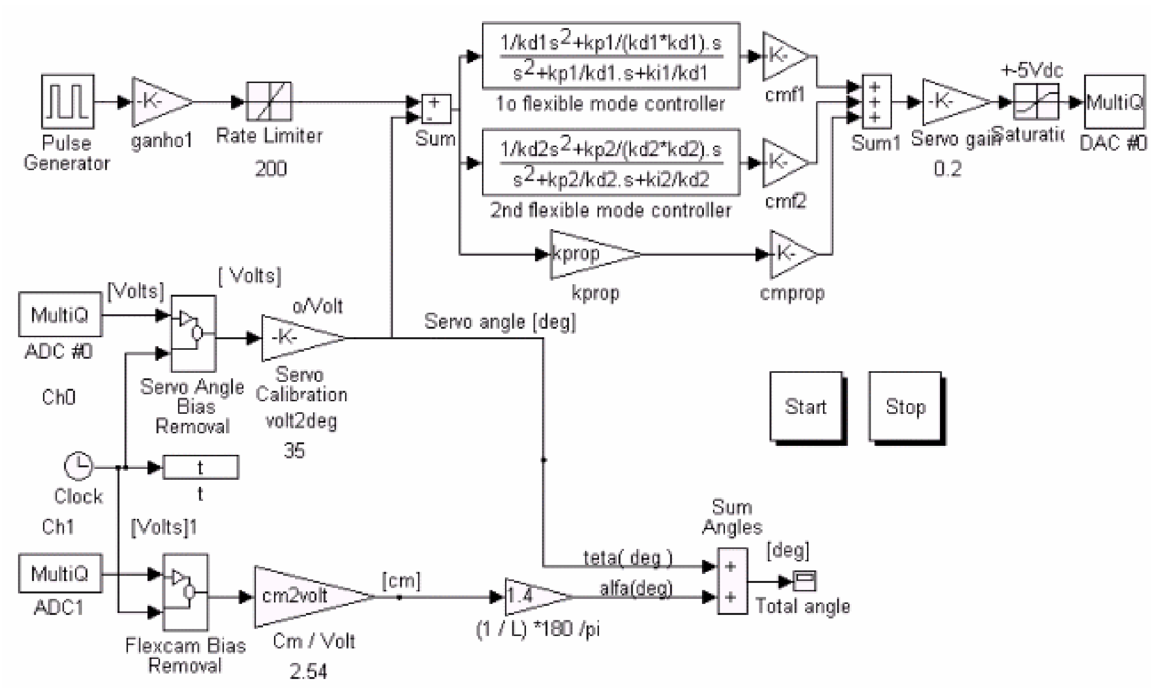

Figure 2. Typical blocks used in Simulink toolbox.

The camera output is an analog signal which is proportional to the relative deflection of the light source from the central axis. The linear displacement y (measurement of tip deflection) corresponds to a linear voltage output. The system parameters are presented in Table 1.

Table 1 – System parameters.

Actuator (Hub SRV-02)		**Flexible Link**	
Parameter	**Numerical value**	**Parameter**	**Numerical value**
Motor torque constant, kt	0.00767 N.m/A	Position sensor gain	0.39 V/cm
Motor torque constant, km	0.00767 V/rd.s	Link rigid body inertia	0.0042 kg.m^2
Armature resistence	2.6 Ohm	Link mass	0.06 kg
Armature inductance	0.18 mH	Link thickness	0.8 mm
Gear ratio	14:1	Link height	0.02 m
Sensitivity	0.0284 V/deg	Link length	0.425 m
Armature inertia	3.87 e-7 kg.m^2	Link mass	0.06 kg

3. HUB MODELING AND IDENTIFICATION PROCESS

The Figure 3a shows the mechanical and electric diagram while Fig. 3b shows the hub Bond-Graphs.

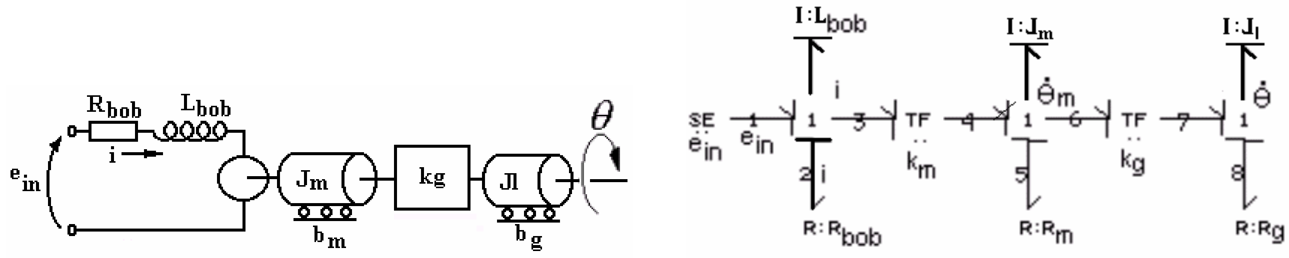

(a) (b)

Figure 3. (a) Hub mechanical and electric diagram and (b) Hub Bond-Graphs

The symbolic state space equation and transfer function were obtained quickly from the augmented Bond-Graphs. Thus, the model to be identified from the input voltage $e_{in}(t)$ to the angular displacement $\theta(t)$ is presented below.

$$\frac{\Theta(s)}{E_{in}(s)} = \frac{1}{(as^2 + bs)} \tag{1}$$

The input-output data were used to identification process of the hub dynamics. It was defined, *a priori*, the sampling frequency f=200Hz (typical bandwith for this servo is 20 Hz). The auto-regressive with exogenous input, ARX model, was used to identify the hub system parameters. The ARX(na,nb,nk) is

$$\begin{aligned}
&A(q)y_k = B(q)q^{-nk}u_k + e_k \\
&A(q) = 1 + a_1 q^{-1} + a_2 q^{-2} + \ldots + a_{na} q^{-na} \\
&B(q) = b_0 + b_1 q^{-1} + b_2 q^{-2} + \ldots + b_{nb} q^{-nb} \\
&y(k) = -a_1 y(k-1) - a_2 y(k-1) - \ldots - a_{ny} y(k-na) + b_1 u(k-1) + b_{nu} u(k-nb) + \nu(k) \\
&\qquad \underline{\theta} = [-a_1 - a_2 \ldots - a_{ny}\ b_1\ b_2 \ldots b_{nu}\ ]^T \qquad \underline{y} = \underline{\underline{X}}\,\underline{\theta} + \underline{\nu} \\
&\qquad \underline{\theta} = \underline{\underline{X}}^{\dagger}\,\underline{y} = \left(\underline{\underline{X}}^T \underline{\underline{X}}\right)^{-1} \underline{\underline{X}}^T\,\underline{y} \qquad \underline{\underline{X}}^{\dagger} = \text{Moore-Penrose Pseudo-inverse Matrix}
\end{aligned} \tag{2}$$

The results encountered using input-output time histories recorded from tests into ARX model, are

$$\hat{G}(s) = \frac{\Theta(s)}{E_{in}(s)} = \frac{377.8}{s(s+42.4)} \tag{3}$$

The Figure 4 shows the output response from tests and the output response obtained from a simulating using the model identified with the same input excitation.

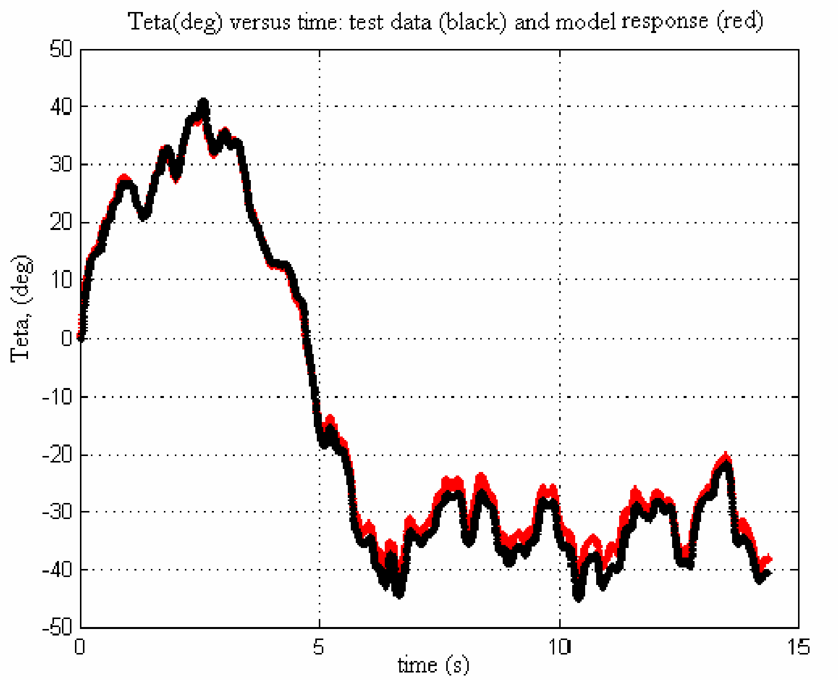

Figure 4. Output time histories comparison

The manufacturer indicates poles $s_1 = 0$ and $s_1 \cong -42$, so the identification is coherent.

4. FLEXIBLE BEAM MODELING AND IDENTIFICATION PROCESS

The Figure 5 shows the physical system, consisting of a hub rotating around z-axis with a cantilevered flexible appendage (beam). The pinned-free boundary conditions are assumed.

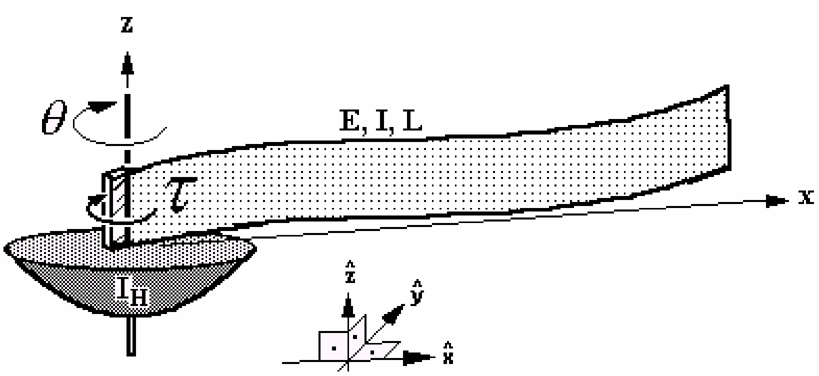

Figure 5. Uniform beam, hub and variables definitions

The equations of motion to the flexible beam are derived using the classical application of Hamilton´s Principle, considering the Euler-Bernoulli assumptions. Thus, the Lagrangian with kinetic and potencial energies is

$$L_g = T - V = \frac{1}{2} I_H \dot{\theta}^2 + \frac{1}{2} \int_0^L \rho \left(\dot{y} + x\dot{\theta} \right)^2 dx - \frac{1}{2} \int_0^L EI \left(\frac{\partial^2 y}{\partial x^2} \right) dx \tag{4}$$

The work performed on the system by the applied torque is

$$W_{nc} = \tau\theta + \tau \frac{\partial y(0,t)}{\partial x} \tag{5}$$

where $\partial y(0,t)/\partial x$ is the angular displacement of the beam on $x = 0$. Applying the Hamilton's principle:

$$\delta \int_{t_1}^{t_2} \left(L_g + W_{nc}\right) dt = 0 \tag{6}$$

and inserting an additional load due to the control's restoring torque applied to the beam at the axis of rotation, according to Barbosa (2001) and Garcia and Inman (1991), we obtain:

$$\begin{cases} EI \dfrac{\partial^4 y}{\partial x^4} + \rho\, \ddot{y} + \rho\, x \ddot{\theta} = \tau \delta'(0) \\ \left(I_H + I_B\right)\ddot{\theta} + \displaystyle\int_0^L \rho\, x\, \ddot{y}\, dx = \tau \end{cases} \tag{7a,b}$$

with the boundary conditions:

$EI \dfrac{\partial^2 y}{\partial x^2}\bigg\|_{x=0} - \tau = 0$,	$y\big\|_{x=0} = 0$	$EI \dfrac{\partial^2 y}{\partial x^2}\bigg\|_{x=L} = 0$	$EI \dfrac{\partial^3 y}{\partial x^3}\bigg\|_{x=L} = 0$
(Balancing torque)	(linear displacement)	(bending moment)	(shearing force)

The solution to flexible displacement of the beam, y, is assumed using a separation of variables, as follows.

$$y(x,t) = \sum_{i=1}^{n} \phi_i(x)\eta_i(t) \tag{8}$$

where n is the number of flexible modes included in the model, and η_i are the modal coordinates. The solution to the angular displacement is assumed as follows, considering the modal amplitudes to the beam rotational movement Θ_i according to Soares (1997).

$$\theta(t) = \sum_{i=1}^{n} \Theta_i \eta_i(t) \tag{9}$$

Substituting Equation (9) into Eq. (7b) we obtain:

$$\Theta_i = -\frac{\rho}{\left(I_H + I_B\right)} \int_0^L x \phi_i dx \tag{10}$$

The expressions of Equations (8) and (9) are inserted in the forced Eq. (7a) and then, we multiply each term by ϕ_j and integrate with respect to x from x=0 to x=L. Finally, using the orthogonality property of the modes, we obtain:

$$m_i \ddot{\eta}_i + k_i \eta_i = \tau \phi_i'(0) \tag{11}$$

with the coefficients

$$m_i = \int_0^L \rho \phi_i \phi_i dx + \int_0^L \rho\, x \phi_i dx \qquad \text{and} \qquad k_i = \int_0^L EI \frac{\partial^4 \phi_i}{\partial x^4} \phi_i dx$$

The Bond-Graph for a beam with force-free boundary conditions is thus linked to the Bond-Graph developed to the hub and presented in Fig. 6.

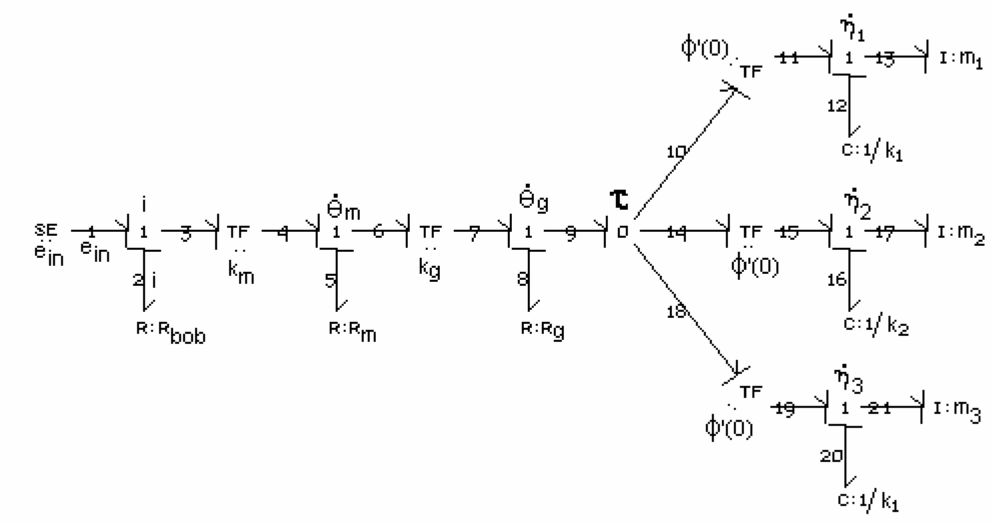

Figure 6. Fully augmented Bond-graph model of the Servo plant and flexible beam

The eigenfunctions and corresponding eigenvalues equations to pinned-free boundary conditions are presented as follow.

$$\phi_i(x) = A_i\left[\frac{\cosh(a_i L)}{\cos(a_i L)}\sin(a_i L) + \sinh(a_i L)\right] \qquad \tan(a_i L) = \tanh(a_i L) \tag{12}$$

The symbolic transfer function $G(s)$, from input voltage $e_{in}(t)$ to the end of the beam $y(L,t)$, is obtained developing the conversion on the state space equations based on the fully augmented Bond-Graph model, shown in Fig. 6. The 6[th] order model to be identified is:

$$G(s) = \frac{Y(L,s)}{E_{in}(s)} = \frac{a_5 s^5 + a_4 s^4 + a_3 s^3 + a_2 s^2 + a_1 s + a_0}{b_6 s^6 + b_5 s^5 + b_4 s^4 + b_3 s^3 + b_2 s^2 + b_1 s + b_0} \tag{13}$$

where the poles are associated to the frequency of vibrations due to first, second and third modes. Inserting the system parameters presented in Table 1, in the symbolic transfer function, Eq. (13), we obtain:

```
                 -3.8e-015 s^5 - 4.91e-005 s^4 + 3.8e-013 s^3 - 0.0117 s^2  + 2.28e-012 s - 0.85
Y(L,s)/Ein(s) =  ---------------------------------------------------------------------------------------
                 s^6 + 1.07e-005 s^5 + 320.699 s^4 + 0.002999 s^3 + 16848.25 s^2  + 0.116 s + 84534.2
```

The frequency response function is plotted in Fig. 7. The zeros, poles and frequencies associated are compiled in Table 2.

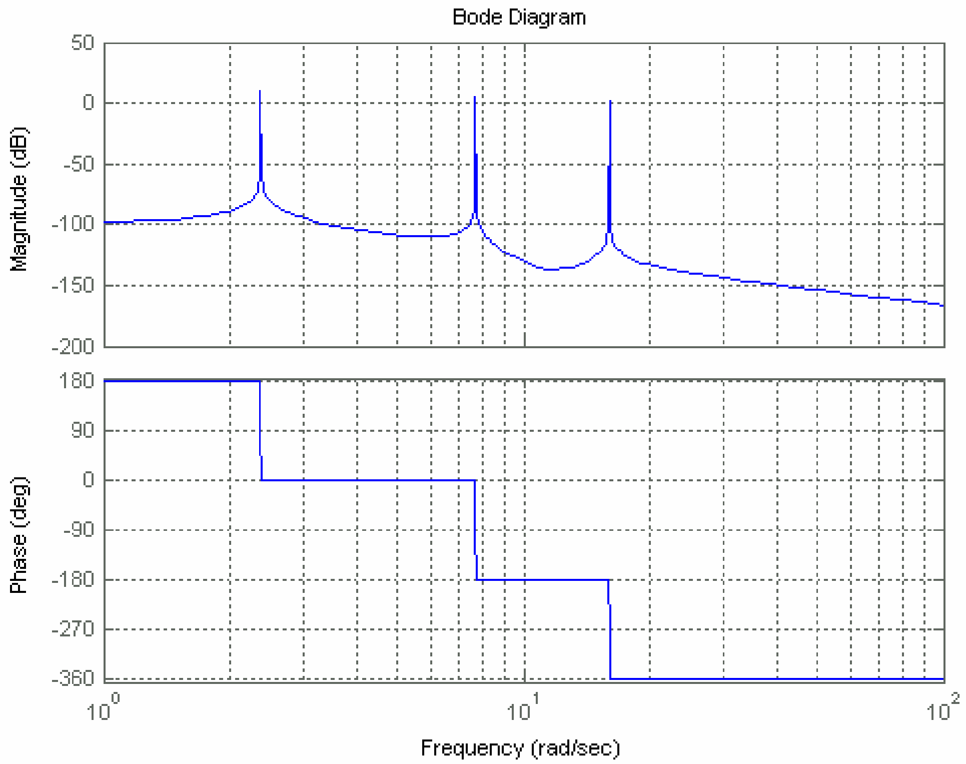

Figure 7. Frequency response function

Table 2 – Zeros, poles and frequencies associated.

Zeros	**poles**	
5 zeros (rd/s)	**6 poles (1/s)**	**frequency (Hz)**
-1.3e+10	-0.0 ± 2.4 i	0.38 Hz
-2.5 ± 11.2i	-0.0 ± 7.7 i	1.23 Hz
2.5 ± 11.2i	-0.0 ± 16.0 i	2.55 Hz

The frequencies associated to the first, second and third modes of vibration can be used to design specific controllers using different strategies.

5. RESULTS COMPARISION

The Figure 8 shows the output autospectrum and Fig. 9 shows the Frequency Response Function (FRF) obtained from two tests. It can be observed that the first, second and third frequencies are coherent. The Table 3 shows the results obtained from three ways: nonparametric, autospectrum and FRF from tests.

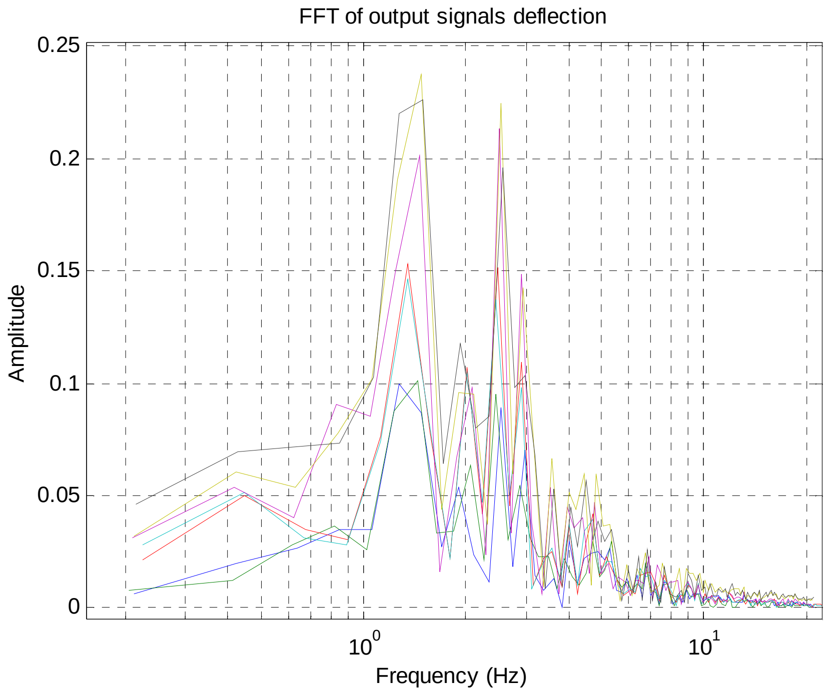

Figure 8. Output deflection autospectrum

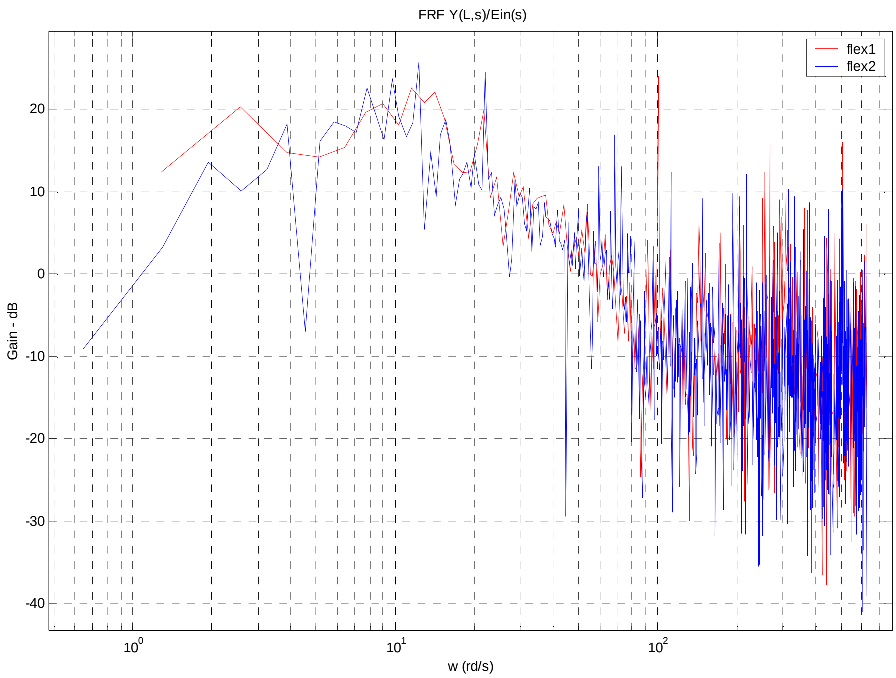

Figure 9. FRF from tests

The Table 3 presents the frequencies and a comparision from methods.

Table 3 – Frequencies of vibrations comparision

Methods	**1st mode**	**2nd mode**	**3rd mode**
Nonparametric	0.38 Hz (2.39 rd/s)	1.23 Hz (7.73 rd/s)	2.55 Hz (16.02 rd/s)
Autospectrum	-	1.1 Hz (6.91 rd/s)	2.2 Hz (13.82 rd/s)
FRF from tests	-	-	2.0 Hz (12.6 rd/s)

7. RECOMMENDATIONS

During the use of FLEXCAM is recommended the camera be aligned in directions that do not have source lights, because this can mask the signals. Frequently is recommended the calibration to the FLEXCAM to obtain the actual camera gain. The sample period shall be chosen as fast as the dominant poles (4 to 20 times due to sampling frequency) to be considered or to identification process. The best flexible models depend on equipment used. So, the use of precision equipment (dynamic analyzer) is recommended. Verify the cables on the back side of the FLEXCAM, they must be free in such way that does not hold the rotating movement of the servo SRV-02.

The choice of location to the source light must be done with care, because it can superimpose two modes of vibration. In Miu (1991) "*If the location of the sensor is exactly at the node, a_r will be identically zero and the resulting transfer zero will superimpose on the second system pole. This pole-zero cancellation has the simple physical meaning that the second mode has become unobservable*".

8. CONCLUSIONS

The main conclusion in this work is that the identified models are coherent and can be used to design a controller to the flexible beam. The ARX model with no polarized signals produced results with quickly convergence. This work presented the modeling and identification of a real flexible plant, via practical results, useful to flexible control designs. Barbosa and Góes (2007) presents a digital controller based on these results and shows good attenuating on the amplitude of vibration, during its movement to a desired angular position.

The FLEXCAM Quanser System was fundamental to the modeling and identification process, as can be verified along this work. The flexibility of using Simulink/Matlab on this test bed is very interesting to study and identify flexible structures.

9. ACKNOWLEDGEMENTS

The first author gratefully acknowledges the cooperation of Carlos H. Silva of IAE/ASE-C Labs. Thanks to Elaine, my little daughter, for the given affection.

10. REFERENCES

Aguirre, L. A. - Introdução à Identificação de Sistemas -Técnicas Lineares e Não-Lineares Aplicadas a Sistemas Reais, - Universidade Federal de Minas Gerais, Editora UFMG, 2000.

Barbieri, E.; Özgüner, Ü. "Unconstrained and constrained mode expansions for a flexible slewing link". Journal of Dynamic Systems, Measurement, and Control, v. 110, p. 417-423, 1988.

Barbosa, E. G., Góes, L. C. S., "Flexible structure control and validation using FLEXCAM QUANSER SYSTEM", Congresso Brasileiro de Engenharia Mecânica, COBEM, Brasil, 2007.

Barbosa, E. G., "Modelagem por Grafos de Ligação de Estrutura Flexível com Atuação Hidráulica", Dissertação de Mestrado, Instituto Tecnológico de Aeronáutica - ITA, Brasil, 2001.

Bendat, J. S., Piersol, A. G. "Random data analysis and measurement procedures". New York, NY.: John Wiley & Sons, 1986. 566 p.

Brandão, M. P. "Fundamentos da dinâmica de estruturas". [S.l.s.n], 1996.

Cadsim Engineering. "CAMP-G: computer aided modeling program with graphical input". Davis: [S,n.], 1999.

Eykhoff, P., System Identification – Parameter and State Estimation, John Wiley & Sons,1979.

Franklin, G. F.; Powell, J. D.; Emami-Naeini, A. "Feedback control of dynamic systems". New York, NY.: Addison Wesley Publishing Company, 1991.

Gani, A., Salami, MJE, Khan R., Active suppression of vibration modes with piezoelectic patches: Modeling, Simulation and Experimentation", Proceedings of the IASTED International Conference, APPLIED SIMULATION AND MODELLING, September 3-5, 2003, Marbella, Spain.

Garcia, E.; Inman, D.J. "Modeling of the slewing control of a flexible structure". Journal of Guidance and Control, v. 14, n. 4, p. 736-742, Jul., 1991.

Goodwin, G. C., Payne, R. L., Dynamic System Identification – Experiment Design and Data Analysis, Academic Press, 1977.

Granda, J. J. "New developments in Bond Graph modeling software tools: the computer aided modeling program CAMP-G and MATLAB". In: IEEE INTERNATIONAL CONFERENCE ON SYSTEMS, Man, And Cybernetics, Hyatt Orlando, Florida, USA, oct., 12-15 1997.

Inman, D. "Vibration with control, measurement, and stability". Englewood Cliffs, NJ.: Prentice Hall, 1989.

Inman, D.J.; Garcia, E. "Modeling of the slewing control of a flexible structure", Journal of Guidance, v. 14, n. 4, p. 736-742, jun., 1988.

Junkins, J. L.; Kim, Y. "Introduction to dynamics and control of flexible structures". Washington, DC: [s. n.], 1993.

Karnopp, D. C.; Margolis D. L.; Rosenberg, R. C. “System dynamics: a unified approach”. New York, NY.: Wiley-Interscience Publication, 1990.
Ljung, L. “Information contents in identification data from closed loop operation”. In: CONFERENCE ON DECISION AND CONTROL, 32nd , 1993, San Antonio. Poceedings... [S.l.s.n.], 1993. p. 2248-2252.
Ljung, L., System Identification – Theory for the user, Prentice-Hall International, New Jersey, USA, 1987.
Mehra, R. K., Nonlinear System Identification: Selected Survey and Recent Trends, 5th IFAC Symp. Identification and systems Parameter Estimation, p. 77- 83, 1979.
Meirovitch, L. “Analytical methods in vibration”. New York, NY.: The Mcmillan Company, 1967. 555 p.
Meirovitch, L. “Dynamics and control of structures”. New York, NY.: John Wiley & Sons, 1989.
Mindlin, R. D. “Influence of rotatory inertia and shear on flexural motions of isotropic, elastic plates”. Journal of Applied Mechanis, v. 18, n. 1, p. 31-38. mar., 1951.
Miu, D., K. “Physical interpretation of transfer function zeros for simple control systems with mechanical flexibilities”. Journal of Dynamic Systems, Measurement, and Control, v. 113, p. 419-424, sep., 1991.
Preumont, A. “Vibration control of active structures: an introduction”. Belgium: Kluwer Academic, 1997.
Quanser Consulting Inc., “A comprehensive and modular Laboratory for Control Systems Design and implementation”, Experimental Workstaions for Feedback Control Eeducation, Toronto, 1997.
Quanser Consulting Inc., “Setting Up Quanser Experiments”, Toronto, 1997.
Ruscio, D. D. “A method for the identification of state space models from input and output measurements”. Journal of Modeling, Identification and Control, v. 16, n. 3, p. 129-143, 1995.
Smith, R. S. “Closed-loop identification of flexible structures: an experimental example”. Journal of Guidance, Control, and Dynamics, v. 21, n. 3, p. 435-440, may., 1998.
Wellstead, P. E. “Introduction to physical system modelling”. London: Academic Press, 1979.

11. RESPONSIBILITY NOTICE

The author(s) is (are) the only responsible for the printed material included in this paper.